Supporting Information

Bimetallic Ir_xPb nanowire networks with enhanced electrocatalytic activity for oxygen evolution reaction

Hangyu Tian[a], Wenlei Zhu[a], Qiurong Shi[a], Shichao Ding[a], Zhaoyuan Lyu[a], Mingjie Xu[b], Xiaoqing Pan[b], Mark H.Engelhard[c], Du Dan[a], Yuehe Lin*[a]

[a]School of Mechanical and Materials Engineering, Washington State University, Pullman, WA, 99164, USA
[b]Irvine Materials Research Institute (IMRI), University of California, Irvine, CA, 92697 USA
[c]Environmental Molecular Sciences Laboratory, Pacific Northwest National Laboratory, Richland, WA, USA

The electrochemical surface area (ECSA) calculation

The ECSA, specific activity (SA) and mass activity (MA) is calculated as follows:

$$ECSA = C_{DL}/(C_s * m_{Ir}) \quad (1)$$

$$i = v * C_{DL} \quad (2)$$

$$SA = i_{@350mV} / ECSA \quad (3)$$

$$MA = i_{@350mV} / m_{Ir} \quad (4)$$

The specific capacitance (Cs) is 0.035 mF cm^{-2} in 0.1M $HClO_4$ aqueous solution and the mass loading (m_{Ir}) of Ir_xPb metallic nanowire networks (MNNs) and commercial IrO_2 is calculated by molecular mass. ECSA is calculated through the equation (1). According to equation (2), the double layer capacitance (C_{DL}) is obtained from the charge current i as function of the scan rate ν, equal to the slope based on the equation (2). The SA and MA is calculated based on equation (3) and (4), involving the current density at an overpotential of 350 mV ($i_{@350mV}$), ECSA and m_{Ir}. The SA is obtained by the division of $i_{@350mV}$ by ECSA and the MA is obtained by the division of $i_{@350mV}$ by m_{Ir}.

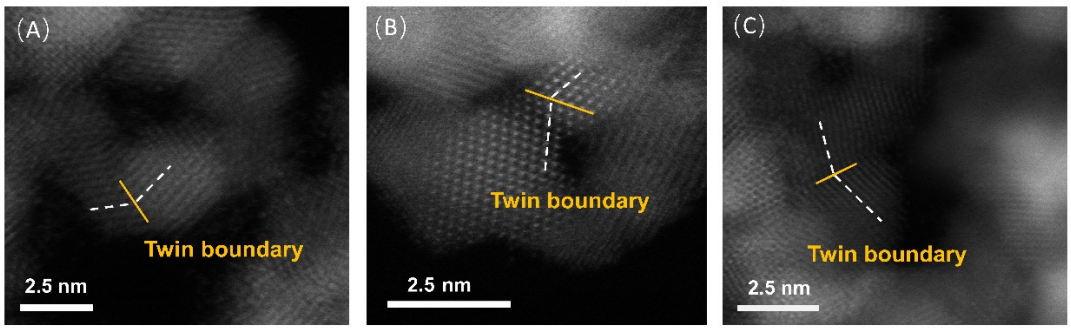

Figure S1. (A-C) HAADF-STEM image of Ir_XPb for twin boundary.

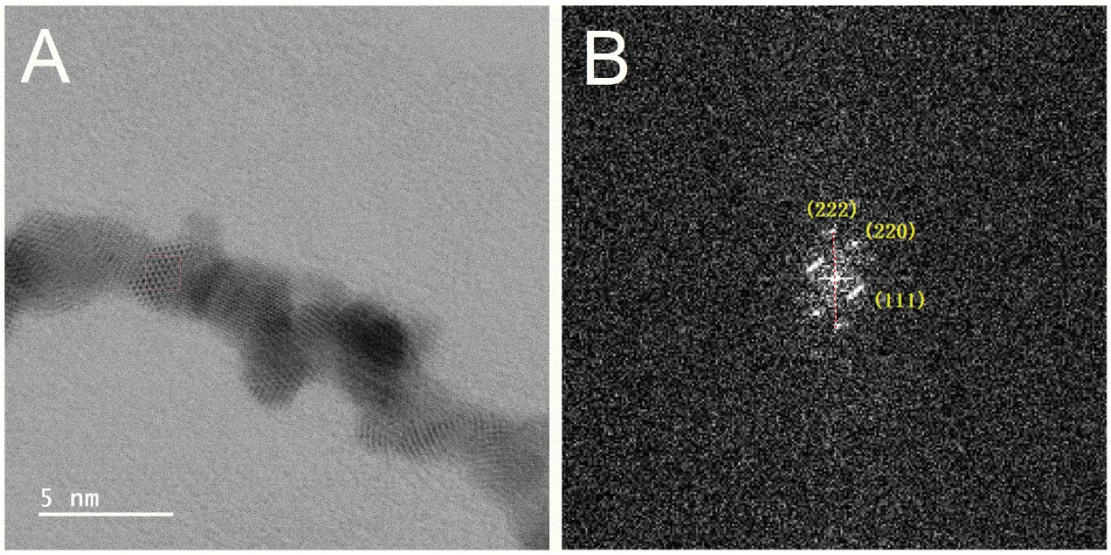

Figure S2. TEM image of Ir_3Pb (a) and corresponding FFT (b).

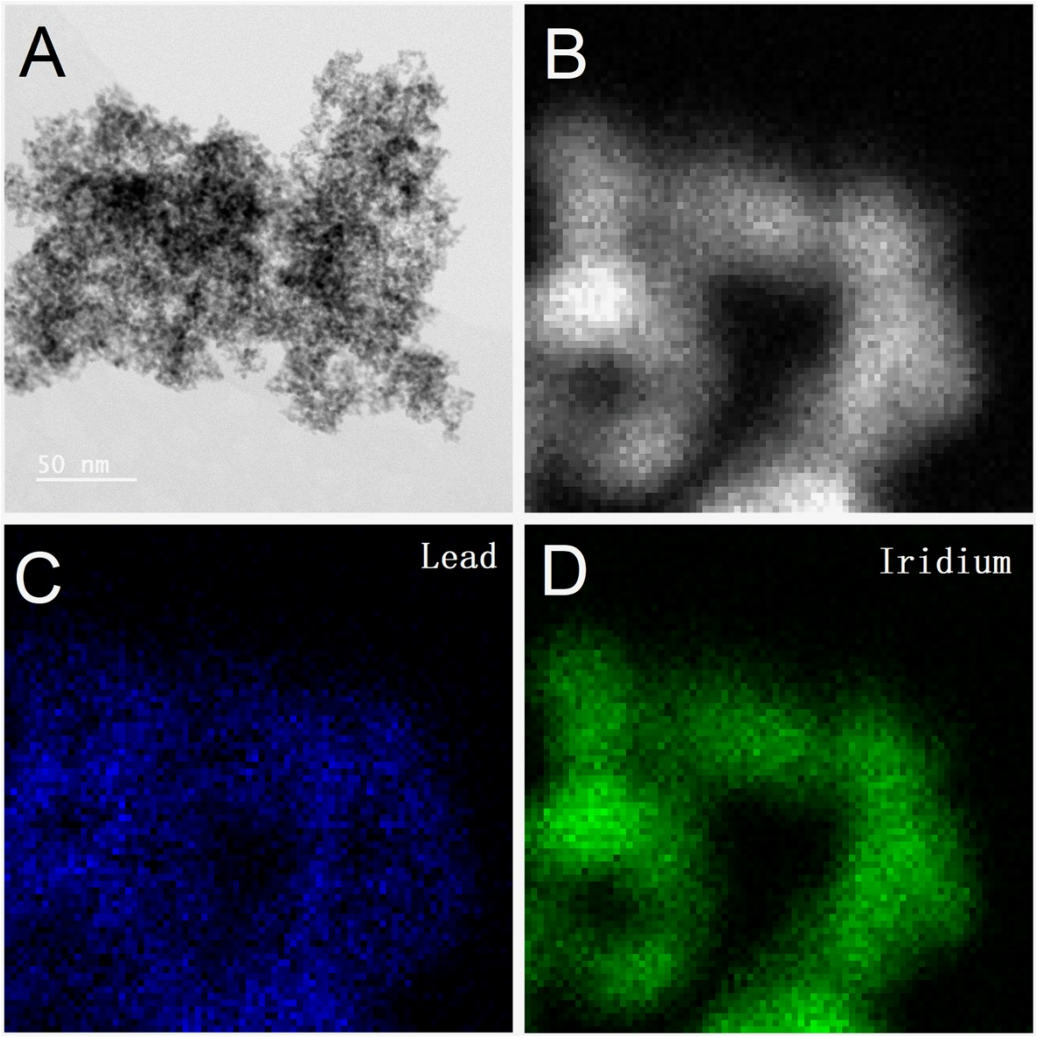

Figure S3. TEM image (a) and HRTEM image (b) of Ir_4Pb.

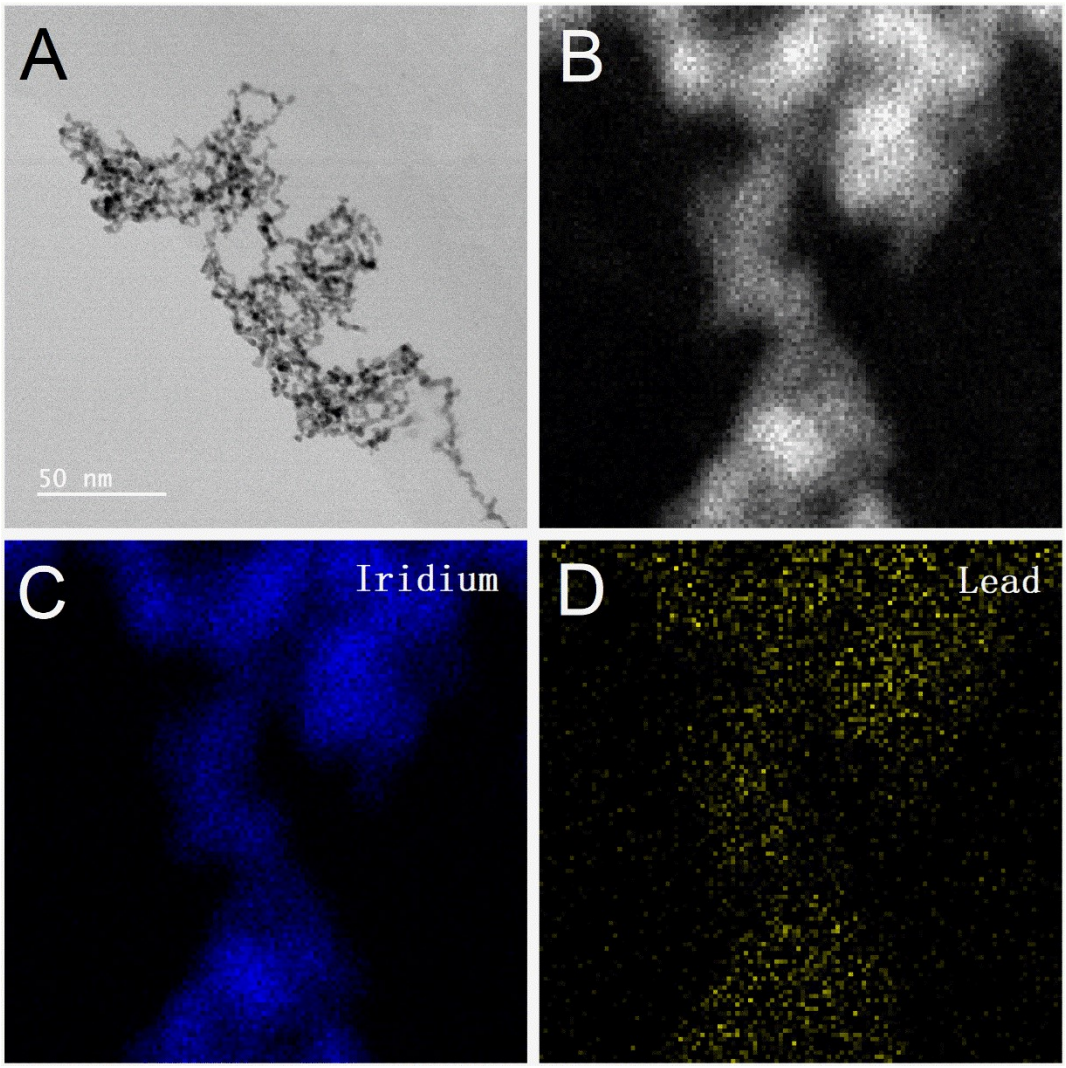

Figure S4. TEM image (a) and HRTEM image (b) of Ir_5Pb.

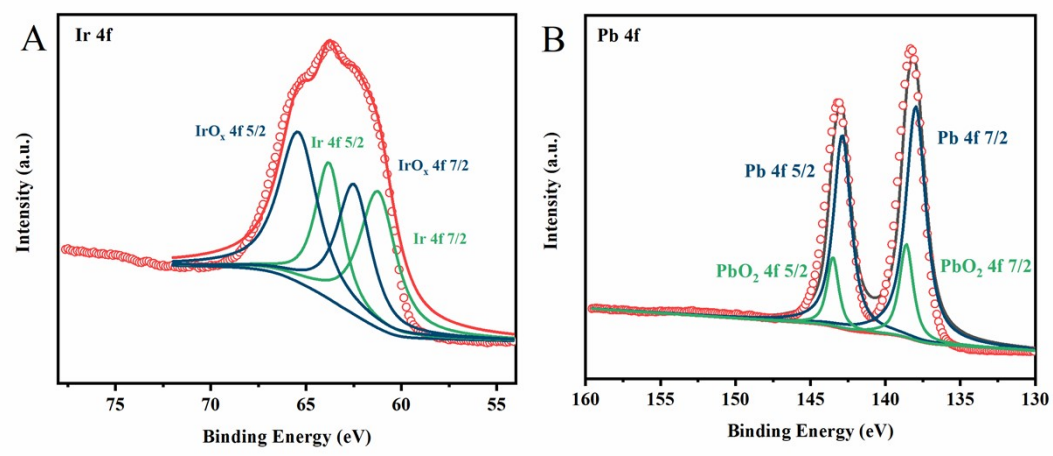

Figure S5. XPS spectra of Ir_3Pb aerogels, corresponding to the 4f peak of Ir (a) and the 4f peak of Pb (b), respectively.

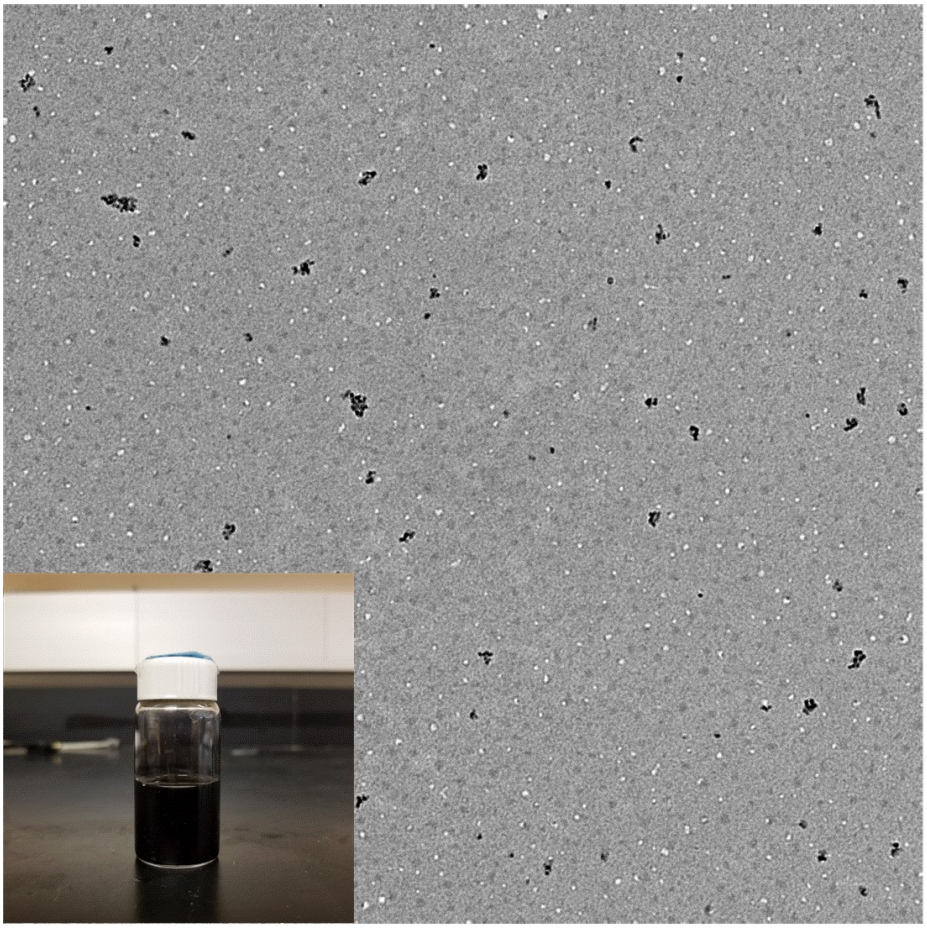

Figure S6. Colloid solution of Ir hydrogel without Pb.

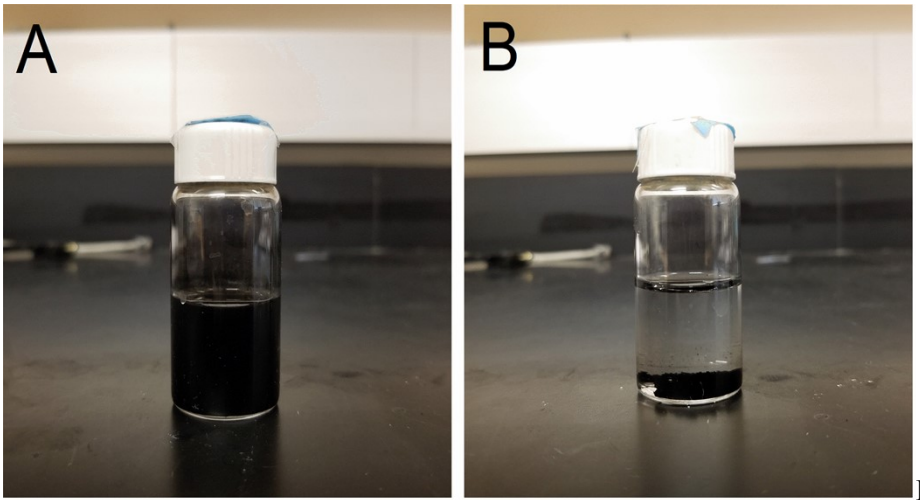

Figure S7. Obtained hydrogel solution without Pb addition (a) and (b) with Pb addition.

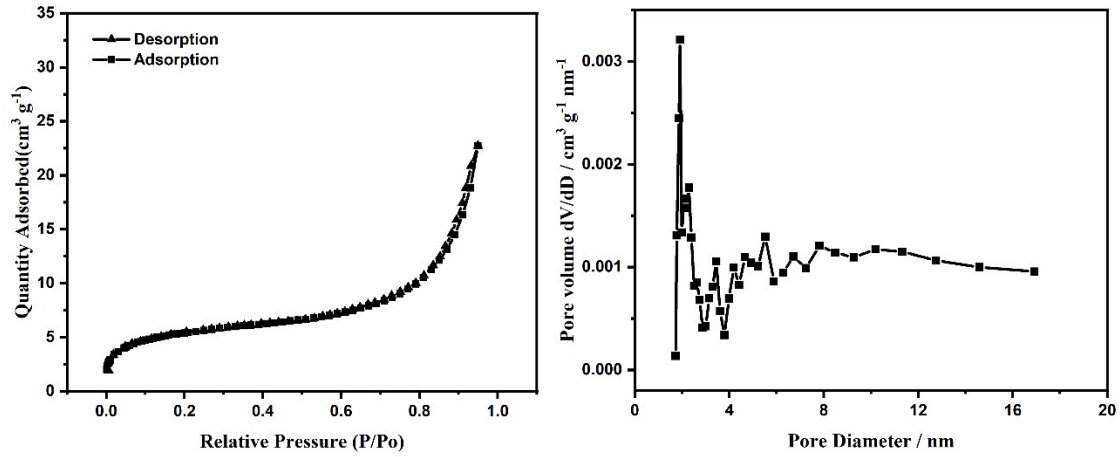

Figure S8. (A) Nitrogen physisorption isotherm. (B) Pore size distribution of prepared Ir_3Pb.

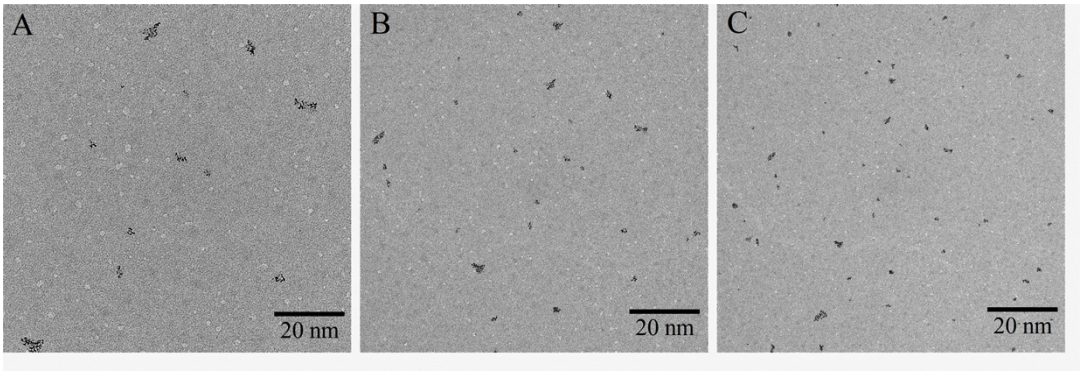

Figure S9. TEM image of Ir_3Pb MNNs at 90 ℃ (A), 120 ℃ (B) and 150 ℃ (C).

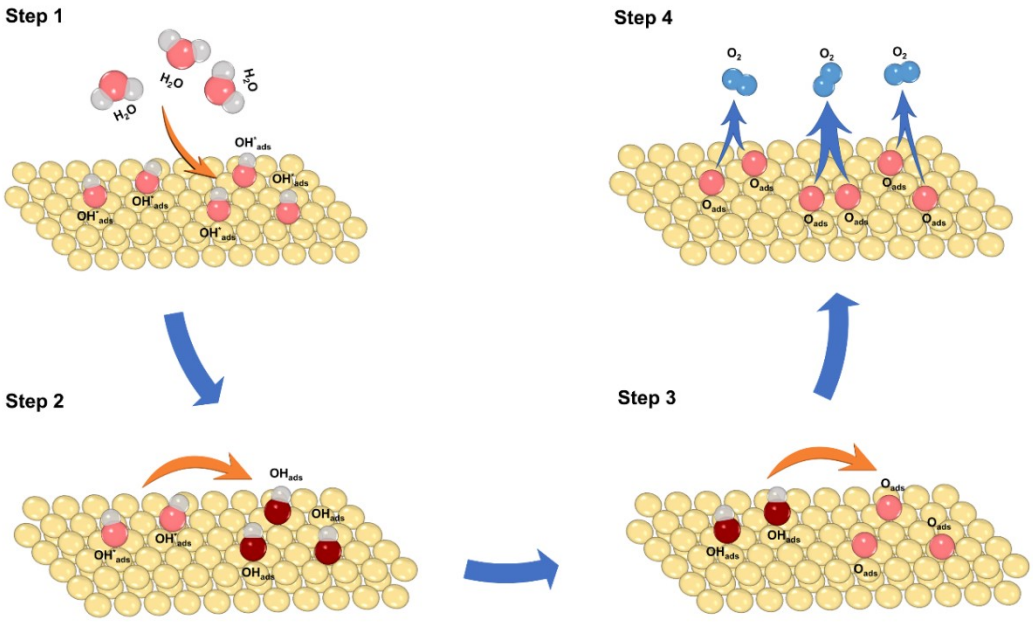

Figure S10. The illustration of OER adsorption mechanism in acid media.

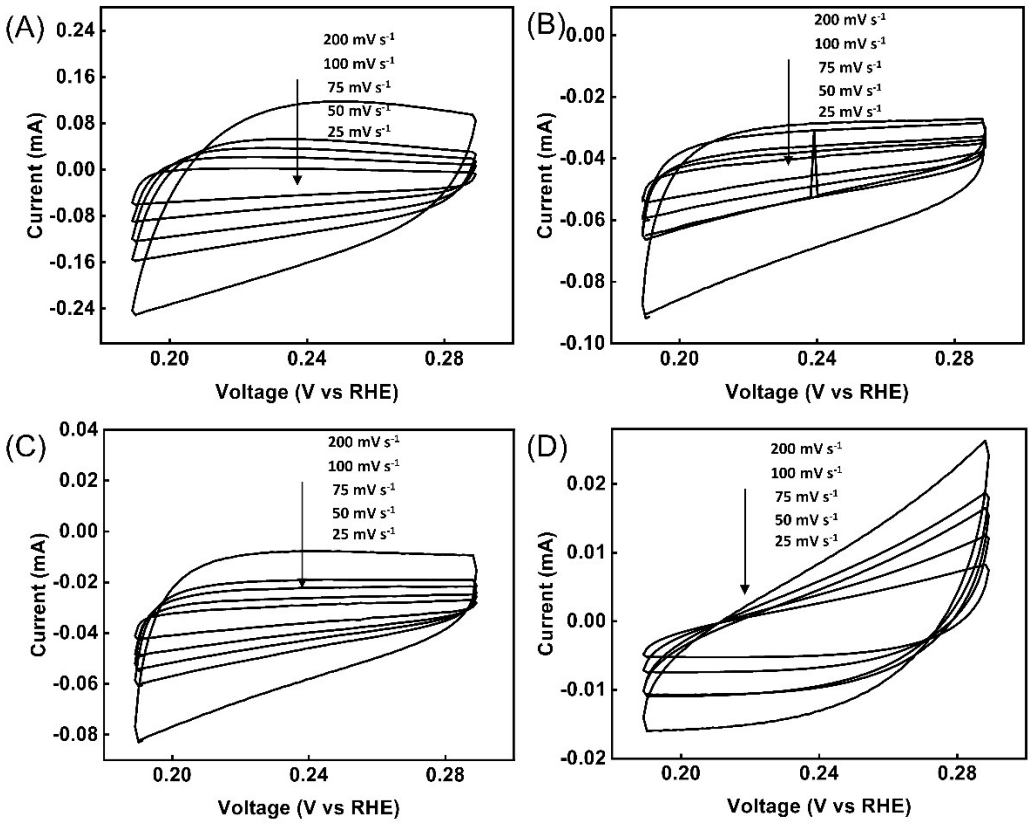

Figure S11. (A-D)The cyclic voltammetry scan of Ir_3Pb, Ir_4Pb, Ir_5Pb and IrO_2 at different scan rates(25 mV/s, 50 mV/s, 75 mV/s, 100 mV/s and 200 mV/s).

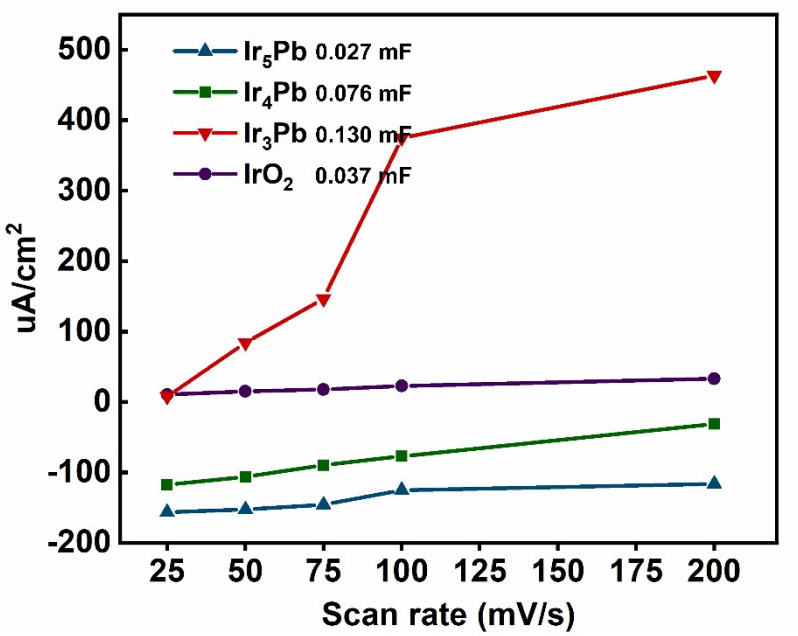

Figure S12. The cathodic charging currents measured at 0.25 V vs. SCE plotted as a function of scan rate.

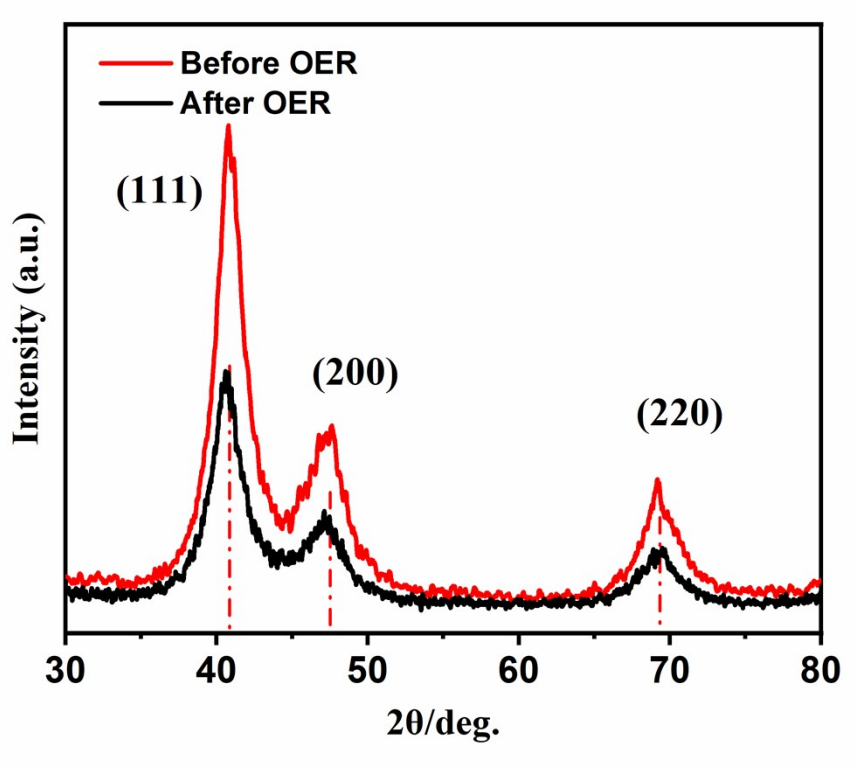

Figure S13. The X-ray diffraction pattern of Ir_3Pb after ADT test.

Table S1. Comparison OER activity of Ir-based electrocatalysts in 0.1M $HClO_4$ acidic solutions at the current density of 10 mA/cm^2.

Ir-based electrocatalysts	Loading of catalysts (ug/cm^2)	Overpotential at 10 mA cm^{-2} (mV)	Reference
$SrCo_{0.9}Ir_{0.1}O_{3-\delta}$	255	320	[1]
IrCoNi nanocrystals	51	303	[2]
Ir Cu nanocrystal	198	311	[3]
$IrNiO_x$ core-shell particles	10.2	280	[4]
IrNiCu double-layered nanoframe	20	303	[5]
AlNiCoIrMo HEA	24.3	275	[6]
Pt-Ir-Pd nanocages	16.8	408	[7]
Bimetallic Ir-Pb Nanowire Networks	25.9	307	This work

Table S2. The ICP-OES results of Ir_xPb MNs.

	Ir (ppm)	Pb (ppm)	Atomic ratio
Ir_5Pb	0.1012	0.0226	5
Ir_4Pb	1.34	0.35	4
Ir_3Pb	0.1787	0.0551	3

Table S3. The ICP-OES results of Ir_xPb MNs after ADT.

	Pb (ppb)	Leaching weight rates(%)
before	0.07	-
after	0.17	0.1

Reference

1 Y. Chen, H. Li, J. Wang, Y. Du, S. Xi, Y. Sun, M. Sherburne, J. W. Ager, A. C. Fisher and Z. J. Xu, *Nat. Commun.*, 2019, **10**, 572.

2 J. Feng, F. Lv, W. Zhang, P. Li, K. Wang, C. Yang, B. Wang, Y. Yang, J. Zhou, F. Lin, G. Wang and S. Guo, *Advanced Materials*, 2017, **29**, 1703798.

3 Y. Pi, J. Guo, Q. Shao and X. Huang, *Chem. Mater.*, 2018, **30**, 8571–8578.

4 H. N. Nong, H.-S. Oh, T. Reier, E. Willinger, M.-G. Willinger, V. Petkov, D. Teschner and P. Strasser, *Angewandte Chemie. Int. Ed.*, 2015, **54**, 2975–2979.

5 J. Park, Y. Sa, H. Baik, T. Kwon, S. Joo and K. Lee, *ACS Nano*, 2017, **11**, 5500–5509.

6 Z. Jin, J. Lv, H. Jia, W. Liu, H. Li, Z. Chen, X. Lin, G. Xie, X. Liu, S. Sun and H. Qiu, *Small*, 2019, **15**, 1904180.

7 J. Zhu, M. Xie, Z. Chen, Z. Lyu, M. Chi, W. Jin and Y. Xia, *Adv. Energy. Mater.*, 2020, **10**, 1904114.